

---

---

PHYSICOCHEMICAL PROBLEMS  
OF MATERIALS PROTECTION

---

---

## Surface Features and Electrochemical Properties of Corrosion Resistant Ni–Ti Coatings

Ramesh S. Bhat<sup>a,\*</sup>, K. B. Manjunatha<sup>b</sup>, and S. Kshama Shetty<sup>c</sup>

<sup>a</sup> Department of Chemistry, NMAM Institute of Technology, Nitte-574110, NITTE (Deemed to be University), Mangalore-575018, Karnataka, India

<sup>b</sup> Department of Physics, NMAM Institute of Technology, Nitte-574110, NITTE (Deemed to be University), Mangalore-575018, Karnataka, India

<sup>c</sup> Department of Chemistry, Nitte Meenakshi Institute of Technology, Bangalore, 560064 India

\*e-mail: rameshbhat@nitte.edu.in

Received December 26, 2021; revised April 27, 2022; accepted May 4, 2022

**Abstract**—Nowadays, application of Ni–Ti alloys is receiving a great interest because of their premium hardness, wear, and corrosion resistance properties. Anti-corrosive Ni–Ti alloy coatings were fabricated by electrodeposition technique. The bath constituents and electrodeposition conditions have been optimized by the Hull cell technique. The surface features of the Ni–Ti alloy coating were analyzed with Scanning electron microscopy (SEM) along with Energy dispersive x-ray spectroscopy (EDX) depicting the presence of Ti, C, Ni, and O elements in the deposit. The phase structure of the alloy coating at different current densities was studied with X-ray diffraction spectroscopy (XRD). The micro-hardness of the coating film was measured by Vicker's micro-hardness tester and the maximum value was found to be 136 HV<sub>0.5</sub> at optimal current density (4 A/dm<sup>2</sup>). The potentiostatic polarization and electrochemical impedance spectroscopy measurements were used to determine the corrosion properties of the Ni–Ti coating films. New low-cost sulphate bath has been proposed for uniform Ni–Ti alloy coating and the results indicate greater corrosion resistance properties, and these coatings can be used for biomedical, electronics and aerospace industries.

**Keywords:** corrosion, electroplating, hardness, additives, electrochemical study, coatings

**DOI:** 10.1134/S2070205122050045

### INTRODUCTION

The interesting field of electrodeposition covers a broad range of technical and engineering activities related to biomedical, rocketry, computers, space technology, etc. In recent years, novel innovations and developments have taken place in this field. For many applications, metals and their alloys are preferred to other materials because of their visual tensile strength, hardness, abrasion resistance, thermal or electrical conductivity, and anti-corrosion properties, etc. Electroplating of thin metal or alloy coatings has become one of the most important techniques used in many industries screening distinctive advantages compared to most other finishing technologies [1]. It is renowned that an active metal such as titanium can reveal a high degree of resistivity against destructive environmental influences. Titanium may reduce destruction cost, save power, avoid product contamination and fight against corrosion [2]. Kremann [3] was the first to do a thorough investigation into the electroplating of alloys and associated processes. Later Brenner's enormous work [4] provided a theoretical ground work for this emerging discipline up to 1960.

Surface modification and specialized treatment of materials can improve their physical properties, wear resistance, corrosion behaviour, and high-temperature stability of substrates for various industrial applications [5–7]. The Ni–Ti coatings have various properties such as biocompatibility, shape memory, better wear resistance, and good corrosion resistance. These alloy coating films have a large number of applications in the fields of biomedical technology, electronics, aerospace, automobile, etc [8–12]. Ni–Ti alloys films have been developed by various methods, such as spraying [13] and laser ablation [14] magnetron sputtering [15], powder metallurgy [16], and electrodeposition techniques [17–19]. Among these techniques, electroplating is of particular importance as a technique for developing various coatings at room temperature, low cost, and elevated deposition rate.

Electroplating is largely dependent on pH of the medium and the time for deposition. Higher the time taken for deposition, greater is the increase in pH leading to the formation of metal hydroxide layer on the substrate affecting the quality of the coating. The factors like temperature, electrolyte concentration, applied potential/current also influences the mor-

**Table 1.** The baths chemical constituents, electroplating conditions, and their values

Bath composition	Amount in g/L	Operating parameters
NiSO <sub>4</sub> ·7 H <sub>2</sub> O	100.0	pH 5.0
TiSO <sub>4</sub>	30.0	Temperature: 30°C
Sodium acetate	65.0	Anode: Pure Nickel
Citric acid	3.0	Current density: 4.0 A/dm <sup>2</sup>
Sulphanilic acid	5.0	

phology of the coating, thickness and hardness and also the electrochemical properties [19–21]. In the present work, Ni–Ti coatings were made on mild steel substrates employing an electroplating process. The effect of current density on composition, surface morphology, phase structure, hardness, and anti-corrosive properties of the coatings were investigated.

#### *Experimental Methodology*

A flat mild steel specimen of approximately  $3 \times 2 = 6$  cm<sup>2</sup> area was taken as cathode and a nickel plate of the same area as an anode. The surface preparation of mild steel for electrodeposition was made by polishing the mild steel on different grades of emery papers (100, 300, 400, 500, 800, and 1200) following which it was rinsed with distilled water and cleaned with trichloroethylene. The electrolytic bath was formulated using research-grade chemicals and double-distilled water.

The pH of the plating bath was optimized to pH 5 by adding the required quantity of dilute sulphuric acid or sodium hydroxide. The experiments were carried out in room temperature (30°C) and manually stirred with a time of 10 min for deposition. After the deposition, the coated substrates were cleaned with distilled water followed by drying. The bath compositions and functioning parameters for Ni–Ti coatings were optimized with the Hull cell method [17]. Sulphanilic acid (SA) is used as an additive for the plating process. Citric acid (CA) serves as a buffer to control the pH and sodium acetate is used as conducting agent. An electroplating cell, of 200 mL capacity was used. The coatings were carried out using a DC power analyzer for 10 min (for comparison purpose). Potentiostat (CH-Instruments) with the standard tri-electrode cell was used to carry out electrochemical studies. The calomel, platinum, and MS were used as a reference, auxiliary and working electrodes, respectively. The corrosion properties of the coatings were conducted, in 3.5% sodium chloride (NaCl) solution by potentiostatic polarization and electrochemical impedance spectroscopy (EIS) techniques. A potential limit of  $\pm 200$  mV from open circuit potential (OCP) was used for polarization study, at a scan rate of 1 mV/s. The frequency range, from 100 kHz to 10 mHz

was used for the EIS study with a perturbation signal of 10 mV. Scanning electron microscopy (SEM), (Model JSM-6380 LA from JEOL), Japan, in the magnification of 1000X was used to observe the surface morphology of the Ni–Ti coatings. The hardness of the coating was measured using a micro-hardness meter. The qualitative composition of metal contents in the coatings was analysed using EDX spectroscopy method. The phase structure of Ni–Ti alloy plating, at different current densities (CDs), was analyzed using XRD (Bruker AXS), using CuK $\alpha$ -radiation, ( $\lambda = 1.5405$  Å, 30 kV).

## RESULT AND DISCUSSION

### *Hull Cell Analysis*

An acid sulphate bath consisting of NiSO<sub>4</sub>, TiSO<sub>4</sub>, Sulphanilic acid, citric acid, and sodium acetate was used for electroplating of Ni–Ti alloy coating. Sodium acetate solution was added to the electrolytic bath to boost the conductivity of the bath. The coating characteristics have been studied in relation to operating parameters and bath composition. The Hull cell approach was used to improve the Ni–Ti bath performance. Table 1 shows the composition and optimal bath conditions for homogeneous Ni–Ti alloy coatings. Except during their fluctuation, all depositions were carried out at a pH of 5 and a temperature of 30°C. For varied current densities (CDs), distinct coatings with different surface appearance were obtained.

### *Hardness and Thickness Analysis*

The Vickers micro-hardness results are given in Table 2. It is clearly seen that the hardness value increases with an increase in applied current density with a load of 500 g. As seen, Ni–Ti coatings hardness value is around 100 HV<sub>500</sub>, which increases to ~136 HV and then decreases to 133 HV on CD range of 1–6 A/dm<sup>2</sup>. The hardness value reaches its maximum value of ~136 HV at the CD of 4 A/dm<sup>2</sup>. The increase in the hardness may be due to Nickel and Ti content in the deposit as reported literatures [17, 22]. At higher CD, the hardness value decreased. A decrease in the

**Table 2.** Effect of current density on hardness, thickness, and electrochemical parameters

CD $i$ , A/dm <sup>2</sup>	VH <sub>500</sub>	Thickness, μm	β <sub>c</sub> , V/dec	β <sub>a</sub> , V/dec	$i_{\text{corr}}$ , μA/cm <sup>2</sup>	$E_{\text{corr}}$ in V, vs. Calomel	CR × 10 <sup>-2</sup> , mm/year
1.0	113	13.3	10.390	13.170	269.2	-1.1041	262.64
2.0	116	15.5	6.430	5.480	100.1	-1.0027	97.69
3.0	127	16.9	9.450	8.840	40.67	-1.0736	39.67
4.0	136	18.1	11.260	8.680	7.848	-1.0340	07.67
5.0	134	19.7	7.607	7.239	23.38	-0.9260	22.81
6.0	133	21.4	7.060	5.646	214.8	-1.0228	209.55

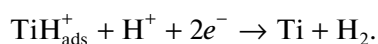
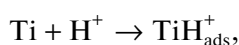
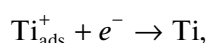
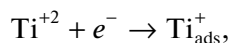
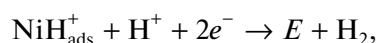
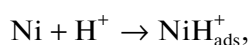
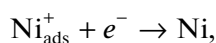
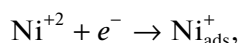
hardness value at 6 A/dm<sup>2</sup> may be attributed to the excessive evolution of hydrogen on cathode resulting in the formation of porous deposit.

As indicated in Table 2, the thickness of the deposit increases with the increase in CD. The linear relationship between deposit thickness and CD could be related to the production of porous metal hydroxide at the cathode because of an increase in pH caused by hydrogen evolution.

#### Mechanism of Electrodeposition

The electrochemical reactions that occur on the cathode surface are detailed in two steps in the mechanism of Ni–Ti coating on mild steel (MS) [23]. On the MS substrate, Ni and Ti ions are deposited. Furthermore, because Ni<sup>+2</sup> ions react with hydrogen ions to generate NiH<sub>ads</sub><sup>+</sup>, secondary reactions must be considered, much as Ti<sup>+2</sup> ions react with hydrogen to form TiH<sub>ads</sub><sup>+</sup>. These intermediate species are produced during the adsorption process and eventually disintegrate to form metallic Ni and metallic Ti.

The electrochemical reactions that occur on mild steel substrate could be described as follows



Ti<sup>+2</sup> and Ni<sup>+2</sup> are dissolved, hydrolyzed or not, as metallic ions. TiH<sub>ads</sub><sup>+</sup> and NiH<sub>ads</sub><sup>+</sup> which may not contain hydroxyl group are adsorbed monovalently in

intermediate reactions. Ti and Ni are the metallic deposits of titanium and nickel, respectively [24–26].

#### Potentiodynamic Polarization Analysis

The potentiodynamic polarization curves of Ni–Ti alloy deposited from a chloride bath were investigated at varied plating current densities ranging from 1.0 to 6.0 A/dm<sup>2</sup>. The polarization investigation was carried out at room temperature and corrosion data presented in Table 2. The polarization curves of different coatings were measured at their open circuit potential (OCP), and corrosion current densities ( $i_{\text{corr}}$ ) and corrosion potentials ( $E_{\text{corr}}$ ) were calculated from the intercepts on the cathodic (β<sub>c</sub>) and anodic (β<sub>a</sub>) Tafel slopes by extrapolation, obtained with reference to the calomel electrode. The polarisation curves at different current densities shown in Fig. 1. The corrosion potentials are directly related to the corrosive activities of the Ni–Ti alloy coating in corrosive media. The coatings corrosion resistance is primarily determined by the deposits structural topography, chemical compositions, and phase structure [27]. The most important cathodic reduction of Ni–Ti alloy is oxygen reduction, which is the rate controlling stage in corrosion [28]. The coatings improved corrosion resistance, on the other hand, corresponds to higher positive corrosion potential ( $E_{\text{corr}}$ ) or lower corrosion current ( $i_{\text{corr}}$ ) values [29]. Table 2 shows that the  $i_{\text{corr}}$  of the Ni–Ti coating decreases with an increase in CDs. However,  $i_{\text{corr}}$  of Ni–Ti alloy plated at 4.0 A/dm<sup>2</sup> exhibits a minor value (7.848 μA cm<sup>-2</sup>). Thus, the raise in applied CD leads to a decrease in  $i_{\text{corr}}$  of the coating and then increased at higher CD, which may be due to non-uniform and porous deposits (Table 2). The least  $i_{\text{corr}}$  at 4 A/dm<sup>2</sup> shows enhanced corrosion resistance. Moreover, Abou-Krishna [30] found that increasing the plating current density, improved Ni content in the coating, which led to higher corrosion resistance properties. Table 2 shows that the corrosion rate of the deposits decreases with an increase in current densities which may be due to a change in the phase structure of the coatings. The corrosion rate was found to be increased at higher current densities (5 A/dm<sup>2</sup>) which

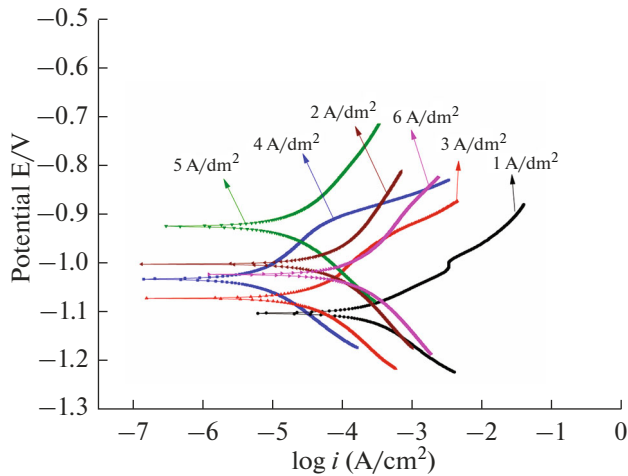


Fig. 1. Tafel plot of Ni–Ti alloy coatings.

may be due to non-uniformity in the deposit (Table 2). The large variation in the Tafel's slope of cathodic polarization, shown in Table 2, indicates that the protection efficacy of the coatings is cathode controlled.

#### Impedance Analysis

Electrochemical impedance spectroscopy (EIS) is a corrosion measurement technique that looks at the characteristics and dynamics of the electrochemical process at the electrode/solution interface in corrosive solutions. The polarization resistance in Nyquist plots matches the shape of a semicircle [31, 32]. Figure 2 depicts the impedance obtained at various current densities. At low CD (1 A/dm<sup>2</sup>), the Ni–Ti coating had a reduced impedance module and the best coating at optimal CD shows a larger impedance module at 4 A/dm<sup>2</sup>. The porous deposit at higher CD shows least impedance module was found at 6 A/dm<sup>2</sup>. It is linked to the formation of an oxide coating in the air by a small arc at high frequencies [33].

#### X-ray Diffraction (XRD) Analysis

The structural analysis of electrodeposited Ni–Ti coating was carried out through X-ray diffraction (XRD) and the spectra of Ni–Ti coatings at different CDs are shown in Fig. 3. The Ni–Ti coatings were developed through a simple electrodeposition technique. The coating thickness increases with current density (Table 1), as a faster rate of Ni-ion reduction and deposition occurred at higher current density resulting in a larger coating thickness. The three peaks at  $2\theta$  values of 45°, 65°, and 82.5° and corresponding peaks are (111), (220), and (211). The highest peak located at  $2\theta \sim 45^\circ$  can be assigned to the Ni (111) plane of face-centered cubic structure and the coating is highly crystalline [34, 35], and one peak at 65° may be due to Ti (220) plane of body-centered cubic struc-

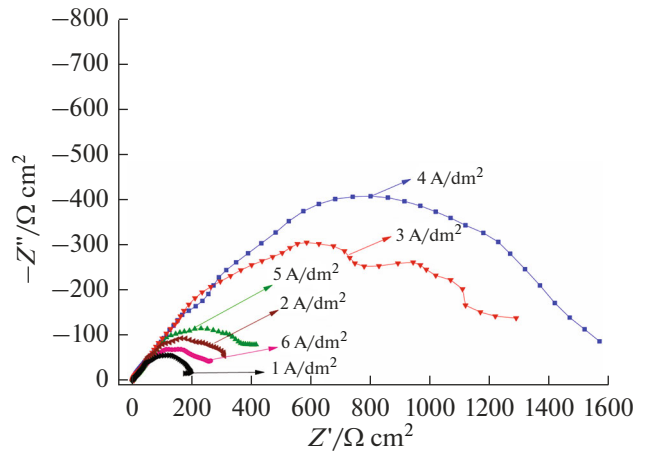


Fig. 2. Nyquist plot of Ni–Ti coating films.

ture [36]. It may be observed that the intensity of peak Ni (111) increases with CD to optimal value and then decreased may be due to the porosity of the deposit. Thus, the XRD study indicates that the drastic increase of corrosion resistance at optimal CD is a result of changes in phase structures of the coating and

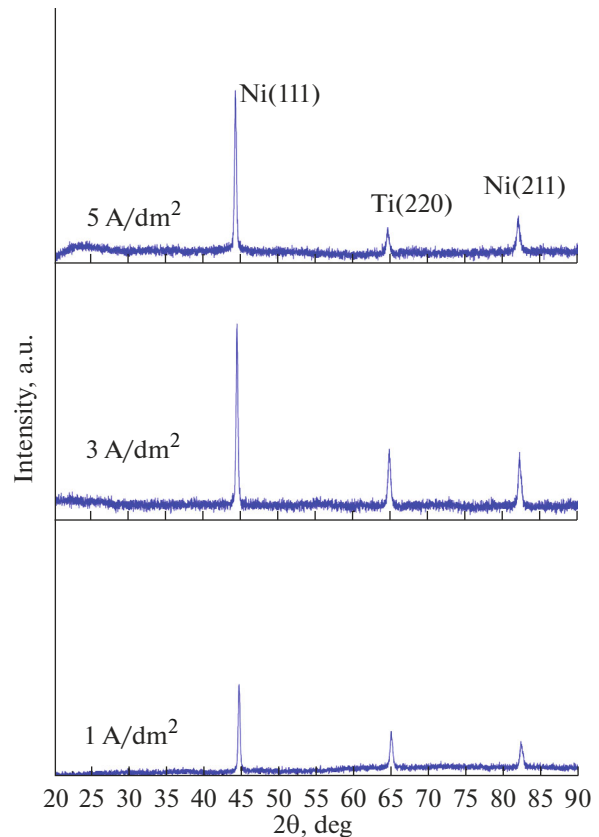


Fig. 3. XRD plot of Ni–Ti alloy coating at different current densities.

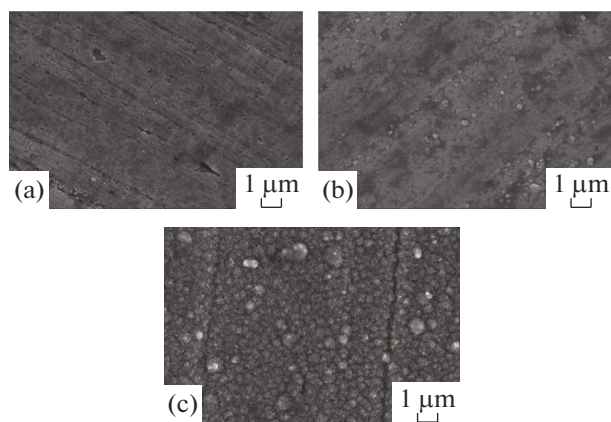


Fig. 4. SEM images of Ni–Ti alloy coatings at different CD's.

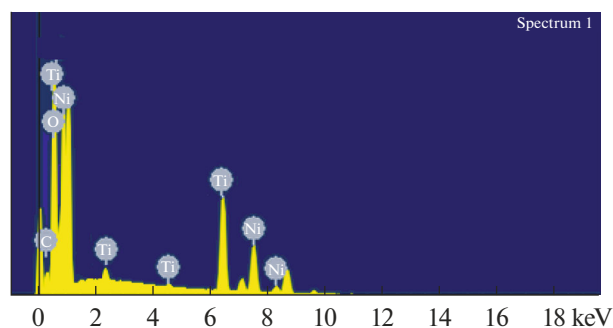


Fig. 5. EDX plot of Ni–Ti coating.

hence better corrosion resistance. Figure 3 shows the Ni and Ti peaks in the coatings, which appear to have no sign of any contamination from other oxide compounds or metallic-compound phases.

### SEM Study

The SEM performance was adopted to understand the surface quality and composition of the Ni–Ti coating obtained at optimal conditions of electrodeposition. The SEM images of Ni–Ti alloy coatings at different current densities as shown in Figs. 4a–4c. At low CD (Fig. 4a), the deposit is non-uniform, greyish, thin, rough surface with irregular deposit was observed and the deposit was uniform with the small grain size of the deposit was found at optimal current density (Fig. 4b) resulted in an increase in Ni and Ti content in the deposit and hence change in phase structure. At higher CD, the deposit was different with a star-like structure with large globule (Fig. 4c) was found may be due to Ti content. The experimental corrosion rate of  $7.67 \times 10^{-2}$  mm/year determined for the Ni–Ti coating is supported by the SEM analysis. EDX (Fig. 5) confirms the presence of Ni (42.05%), Ti (1.35%), C (7.09%) and O (49.51%) elements in the Ni–Ti coatings.

### CONCLUSIONS

In summary, the process parameters have been optimized to achieve high corrosion resistance Ni–Ti alloy coatings. At the optimum current density, the deposit exhibits structurally uniform coating. The corrosion rate was calculated to be  $7.67 \times 10^{-2}$  mm/year at the optimized current density of 4 A/dm<sup>2</sup>. Potentiodynamic polarization and EIS measurement results reveal the significant role of Ni and Ti in the deposit to minimizing the corrosion rate. The hardness and thickness of the deposits are directly proportional to the percentage of Ni and Ti in the coatings. The XRD results revealed that Ni (111) was the dominant phase responsible for improved corrosion resistance. The surface topography of Ni–Ti coatings was confirmed by SEM analysis, revealing the causes for the coating's improved corrosion resistance. Therefore, it is clearly indicated that Ni–Ti alloy coatings may find potential applications in the biomedical, electronics, and aerospace industries.

### ACKNOWLEDGMENTS

The authors gratefully acknowledge Raman Research Institute (RRI), for providing the Instrumental facilities.

### CONFLICT OF INTEREST

The authors declare that they have no conflicts of interest.

### REFERENCES

1. Bajat, J.B., Stankovic, S., Jokic, and B.M., *J. Solid State Electrochem.*, 2009, vol. 13, p. 755.
2. Srivastava, S.K., *Int. J. Res.*, 2020, vol. 7, no. 11, p. 7073.
3. Kremann, R., *Die elektrolytische Darstellung von Lagerungen aus wasserigen Losungen*, Braunschwei: F. Vieweg, 1914.
4. Brenner, A., *Electrodeposition of Alloy, Principles and Practice*, New York: Academic Press, 1963, vol. 2.
5. Shahini, A., Yazdimamaghani, M., Walker, K., Eastman, M., Hatami-Marbini, H., Smith B., et al., *Int. J. Nanomed.*, 2014, vol. 9, p. 167.
6. Yazdimamaghani, M., Razavi, M., Vashae, D., et al., *Surf. Eng.*, 2014, vol. 30, p. 920.
7. Kuru, H., Kockar, H., Alper, M., et al., *J. Magn. Mater.*, 2015, vol. 377, p. 59.
8. Elahinia, M.H., Hashemi, M., Tabesh, M., and Bhaduri, S.B., *Prog. Mater. Sci.*, 2012, vol. 57, no. 5, p. 911.
9. Toker, S.M., Canadinc, D., Maier, H.J., and Birer, O., *Mater. Sci. Eng., C*, 2014, vol. 36, no. 1, p. 118.
10. Fernandes, F.M.B., Mahesh, K.K., Martins, R.M.S., Silva, R.J.C., Baetz, C., and Von Borany, J., *Mater. Charact.*, 2013, vol. 76, p. 35.
11. McMahon, R.E., Ma, J., Verkhoturov, S.V., et al., *Acta Biomater.*, 2012, vol. 8, no. 7, p. 2863.

12. Fadlallah, S.A., El-Bagoury, N., Gad El-Rab, S.M.F., Ahmed, R.A., and El-Ousamii, G., *J. Alloys Compd.*, 2014, vol. 583, p. 455.
13. Tria, S., Elkedim, O., Hamzaoui, R., et al., *Powder Technol.*, 2011, vol. 210, no. 2, p. 181.
14. Sharma, S.K. and Mohan, S., *J. Alloys Compd.*, 2014, vol. 592, p. 170.
15. Zhang, L., Xie, C., and Wu, J., *Mater. Charact.*, 2007, vol. 58, no. 5, p. 471.
16. Tosun, G., Ozler, L., Kaya, M., and Orhan, N., *J. Alloys Compd.*, 2009, vol. 487, no. 1, p. 605.
17. Kanani, N., *Electroplating - Basic Principles, Processes and Practice*, Berlin: Elsevier, 2006.
18. Bhat, R., Bhat, U.K., and Hegde, A.C., *Prot. Met. Phys. Chem. Surf.*, 2011, vol. 47, p. 645.
19. Bhat, R.S. and Shet, V.B., *Surf. Eng.*, 2020, vol. 36, p. 429.
20. Moravej, M., Amira, S., Prima, F., et al., *Mater. Sci. Eng., B*, 2011, vol. 176, p. 1812.
21. Bhat, R., Bekal, S., and Hegde, A.C., *Anal. Bioanal. Electrochem.*, 2018, vol. 10, no. 12, p. 1562.
22. Yusuf, M.M., Radwan, A.B., Shakoor, R.A., et al., *Appl. Electrochem.*, 2018, vol. 48, no. 4, p. 391.
23. Vasilache, V., Gutt, G., Vasilache, T., and Sandu, I., *Rev. Chim. (Bucharest, Rom.)*, 2009, vol. 60, p. 15.
24. Mohanty, U.S., Tripathy, B.C., Das, S.C., and Mishra, V.N., *Metall. Mater. Trans. B*, 2005, vol. 36, p. 737.
25. Soares, M.E., Souza, C.A.C., and Kuri, S.E., *Surf. Coat. Technol.*, 2006, vol. 201, p. 2953.
26. Bhat R. S., Nagaraj P. and Sharada Priyadarshini, *Surf. Eng.*, 2021, vol. 37, no. 6, p. 755.
27. Bhat, R.S., Shetty, S.M., and Kumar, N.A., *J. Mater. Eng. Perform.*, 2021, vol. 30, p. 8188. <https://doi.org/10.1007/s116651>
28. Mansfeld, F., Shih, H., Tsai, C.H., and Greene, H., *Am. Soc. Test. Mater.*, 1993, vol. 1188, p. 37.
29. McCafferty, E., *Corros. Sci.*, 2005, vol. 47, p. 3202.
30. Gelman, D., Starosvetsky, D., and Ein-Eli, Y., *Corros. Sci.*, 2014, vol. 82, p. 271.
31. Abou-Krishna, M.M., *J. Coat. Technol. Res.*, 2012, vol. 9, no. 6, p. 775.
32. Tozar, A. and Karahan, I.H., *Appl. Surf. Sci.*, 2014, vol. 318, p. 15.
33. Winiarsiki, J., Tylus, W., Winiarska, K., and Szczygiel, B., *Corros. Sci.*, 2009, vol. 51, p. 1251.
34. Yang, Y., et al., *Appl. Nanosci.*, 2011, vol. 1, no. 1, p. 19.
35. Dini, J.W., *Electrodeposition: The Materials Science of Coatings and Substrates*, Park Ridge, NJ: Noyes Publ., 1993.
36. Mokgalaka, M.N., Pityana, S.L., Popoola, P.A.I., and Mathebula, T., *Adv. Smart Mater. Appl.*, 2014, vol. 2014, p. 363917. <https://doi.org/10.1155/2014/363917>